Gain of function in the immune system caused by a ryanodine receptor 1 mutation

Mirko Vukcevic[1], Francesco Zorzato[1,2], Simone Keck[3], Dimitrios A. Tsakiris[4], Jennifer Keiser[5], Rick M. Maizels[6] and Susan Treves[1,2,*]

[1]Departments of Anaesthesia and Biomedicine, Basel University Hospital, Hebelstrasse 20, 4031 Basel, Switzerland
[2]Department of Life Sciences and Biotechnology, University of Ferrara, 44121 Ferrara, Italy
[3]Laboratory of Transplantation Immunology, Departments of Biomedicine and Nephrology, University Hospital Basel and University of Basel, Hebelstrasse 20, CH-4031 Basel
[4]Department of Haematology, University Hospital Basel, CH-4031 Basel, Switzerland
[5]Department of Epidemiology and Public Health, Swiss Tropical and Public Health Institute, PO Box, CH-4002 Basel, Switzerland
[6]Institute of Immunology and Infection Research, University of Edinburgh, West Mains Road, Edinburgh EH9 3JT, UK
*Author for correspondence (susan.treves@unibas.ch)

Accepted 1 May 2013
Journal of Cell Science 126, 3485–3492

doi: 10.1242/jcs.130310

Summary

Mutations in *RYR1*, the gene encoding ryanodine receptor 1, are linked to a variety of neuromuscular disorders including malignant hyperthermia (MH), a pharmacogenetic hypermetabolic disease caused by dysregulation of Ca^{2+} in skeletal muscle. *RYR1* encodes a Ca^{2+} channel that is predominantly expressed in skeletal muscle sarcoplasmic reticulum, where it is involved in releasing the Ca^{2+} necessary for muscle contraction. Other tissues, however, including cells of the immune system, have been shown to express ryanodine receptor 1; in dendritic cells its activation leads to increased surface expression of major histocompatibility complex II molecules and provides synergistic signals leading to cell maturation. In the present study, we investigated the impact of an MH mutation on the immune system by studying the $RYR1_{Y522S}$ knock-in mouse. Our results show that there are subtle but significant differences both in resting 'non-challenged' mice as well as in mice treated with antigenic stimuli, in particular the knock-in mice: (i) have dendritic cells that are more efficient at stimulating T cell proliferation, (ii) have higher levels of natural IgG_1 and IgE antibodies, and (iii) are faster and more efficient at mounting a specific immune response in the early phases of immunization. We suggest that some gain-of-function MH-linked *RYR1* mutations might offer selective immune advantages to their carriers. Furthermore, our results raise the intriguing possibility that pharmacological activation of RyR1 might be exploited for the development of new classes of vaccines and adjuvants.

Key words: Ryanodine receptor, RyR1, Dendritic cell, Immune system

Introduction

The ryanodine receptor (RyR1) intracellular Ca^{2+} channel is preferentially expressed in skeletal muscle where it plays a central role in excitation-contraction coupling by releasing Ca^{2+} from the sarcoplasmic reticulum. Recently it was shown that RyR1s are also expressed in other cell types, including neurons, smooth muscle cells and immune cells, specifically in B-lymphocytes and dendritic cells (DC) (Sei et al., 1999; Girard et al., 2001; Bracci et al., 2007; Uemura et al., 2007; O'Connell et al., 2002). DCs are the most potent antigen presenting cells connecting innate and adaptive immunity. They are located in peripheral tissues where they continuously sample the environment for the presence of foreign antigens; when these are encountered DCs process them and then migrate to secondary lymphoid organs where they present the processed antigens in conjunction with major histocompatibility complex II (MHCII) molecules to T-lymphocytes and initiate a specific immune response (Banchereau et al., 2000). Studies on the role of RyR1 in immune cells *in vitro* has established that in B-lymphocytes its activation is coupled to cytokine release (Girard et al., 2001) whereas in DCs it leads to enhanced maturation, release of pro-inflammatory cytokines and enhanced ability to prime T-cells (Bracci et al., 2007).

In humans, mutations in *RYR1* are associated with several neuromuscular disorders, including Malignant Hyperthermia, Central Core disease, some forms of multi-minicore disease, centronuclear myopathy and congenital fibre type disproportion. More than 200 causative mutations have been identified in patients and though they have not all been characterized functionally, malignant hyperthermia (MH) causative mutations are characterized by 'gain of function', whereby they increase the sensitivity of the RyR1 Ca^{2+} channel to activation (Treves et al., 2008; Robinson et al., 2006). Indeed MH Susceptibility (MHS) is characterized by abnormal release of Ca^{2+} from the sarcoplasmic reticulum, metabolic acidosis, increase in body temperature and rhabdomyolysis after contact with a trigger agent. To date the functional effects of *RYR1* mutations have been extensively studied in muscle cells and more recently, in the central nervous system (De Crescenzo et al., 2012) but no data is available on if and how mutations in *RYR1* affect the immune system. In the present study, we analysed the general characteristics of the immune system of a mouse model knocked in for the $RYR1_{Y522S}$ mutation, a mutation that in humans has been shown to be causative of MH. Indeed mice carrying the mutation at the heterozygous state (HET $RYR1_{Y522S}$) are MHS, heat intolerant and develop an MH reaction when exposed to anaesthetics,

whereas at the homozygous state the mutation causes death soon after birth possibly due to breathing impairment (Chelu et al., 2006). Our results show that there are subtle differences in the immune system of the heterozygous $RyR1_{Y522S}$ knock-in mice compared to their wild-type littermates, even in non immunized animals; specifically their DCs have a more mature phenotype, are more potent at stimulating T-cells and the serum concentrations of circulating natural IgG_1 and IgE are significantly increased. Moreover, following a primary antigenic challenge, heterozygous $RYR1_{Y522S}$ mice produce higher levels of antigen-specific IgG. These results support the intriguing possibility that some *RYR1* mutations exert beneficial effects on the immune system.

Results

Phenotypic and functional characteristic of dendritic cells from the HET $RYR1_{Y522S}$ knock-in mouse

It has previously been shown that human monocyte-derived DCs and mouse bone marrow-derived DC express RyR1 (Bracci et al., 2007; O'Connell et al., 2002). In this study we isolated CD11c+ cells from mouse spleens and confirm the presence of the RyR1 transcript. As shown in Fig. 1A, RYR1 transcripts in DCs from wild-type (WT) and heterozygous (HET) $RYR1_{Y522S}$ knock-in mice differ, as the presence of the T>C substitution results in the appearance of a BlpI restriction site in the HET $RYR1_{Y522S}$ mice (Chelu et al., 2006). The presence of the *RYR1* MH-causing mutation in DCs caused a small but significant increase in the resting $[Ca^{2+}]_i$ (Fig. 1B) as well as a significant increase in the surface expression of the maturation marker CD83 (Fig. 1C). An increase in CD83 surface expression could be induced in DCs from WT mice by stimulation with 10 mM caffeine (inset Fig. 1C), indicating that DCs are endowed with a pool of CD83 molecules that can be expressed on the plasma membrane by RyR1 activation. Fig. 1D shows results obtained by real-time PCR of common DC maturation markers; the relative expression of CD83, CD86, IL-12 and IL-23 do not differ between HET $RYR1_{Y522S}$ and WT littermates, indicating that the presence of the mutation does not affect transcription of these genes but rather affects the Ca^{2+}-dependent release of CD83 onto the plasma membrane.

We next investigated if the increase in CD83 surface expression in DCs from the HET $RYR1_{Y522S}$ mice was paralleled by functional changes, as monitored by the mixed lymphocyte reaction. DCs were isolated from spleens of either WT or HET $RYR1_{Y522S}$ littermates (both having the C57BL/6 background) and incubated with different amounts of T-cells from Balb/c mice. The capacity of DCs to stimulate T-cell proliferation was assayed by measuring $[^3H]$thymidine incorporation. As shown in Fig. 2A starting from a DC:T-cell ratio of 1:20, cells isolated from HET $RYR1_{Y522S}$ (grey bars) mice were significantly more efficient at stimulating alloreactive T cell proliferation compared to cells from their WT littermates. Furthermore, supernatants collected 72 h after co-culture of T cells and DCs from the HET $RYR1_{Y522S}$ mice contained significantly higher levels of IFN-γ, with no difference in the

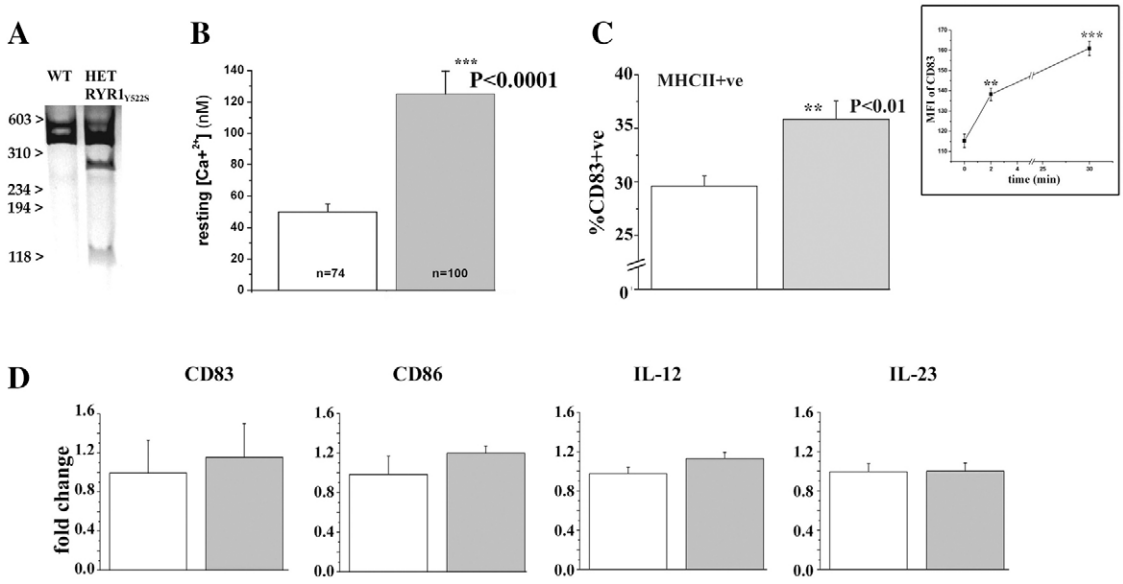

Fig. 1. Expression of $RYR1_{Y522S}$ in mouse CD11c-positive spleen DCs affects the resting $[Ca^{2+}]_i$ and the expression of the maturation marker CD83. (**A**) Total RNA was extracted from purified DCs and the expression of RyR1 was evaluated by RT-PCR as described in Materials and Methods. Digestion of the RyR1 cDNA from wild-type mice (WT) yields the uncut band of about 376 bp, whereas digestion of the cDNA from heterozygous mice (HET $RYR1_{Y522S}$) yields two bands of 276 bp and 100 bp plus the uncut 376 bp band from the wild-type allele. (**B**) The resting $[Ca^{2+}]$ of DCs from HET $RYR1_{Y522S}$ mice is significantly higher than that of their WT littermates (Student's *t*-test, $***P<0.0001$). Fluorescence measurements were performed on single DCs loaded with the ratiometric Ca^{2+} indicator fura-2; results show the mean (±s.d.) intracellular free $[Ca^{2+}]$ (nM) of 74 WT (white bars) and 100 (HET $RYR1_{Y522S}$, grey bars) cells. (**C**) CD11c-positive DCs were isolated from the spleens of WT and HET $RYR1_{Y522S}$ littermates and the percentage of CD83-positive DCs was determined by flow cytometry and is significantly higher in the $RYR1_{Y522S}$ mice (Student's *t* test, $*P<0.01$). The inset shows that treatment of DCs from WT mice with 10 mM caffeine significantly increases surface CD83 expression. Results represent the mean fluorescence intensity values from experiments on four mice, performed in duplicate (ANOVA followed by Bonferroni's post hoc test; $**P<0.0001$, $***P<0.0000002$). (**D**) Real-time PCR for the indicated maturation markers was performed on DCs from WT (empty bars) and HET $RYR1_{Y522S}$ (grey bars) mice. Boxes represent the mean (±s.e.m.) fold increase of four different experiments carried out on CD11c-positive cells from different mice. Results were not statistically different.

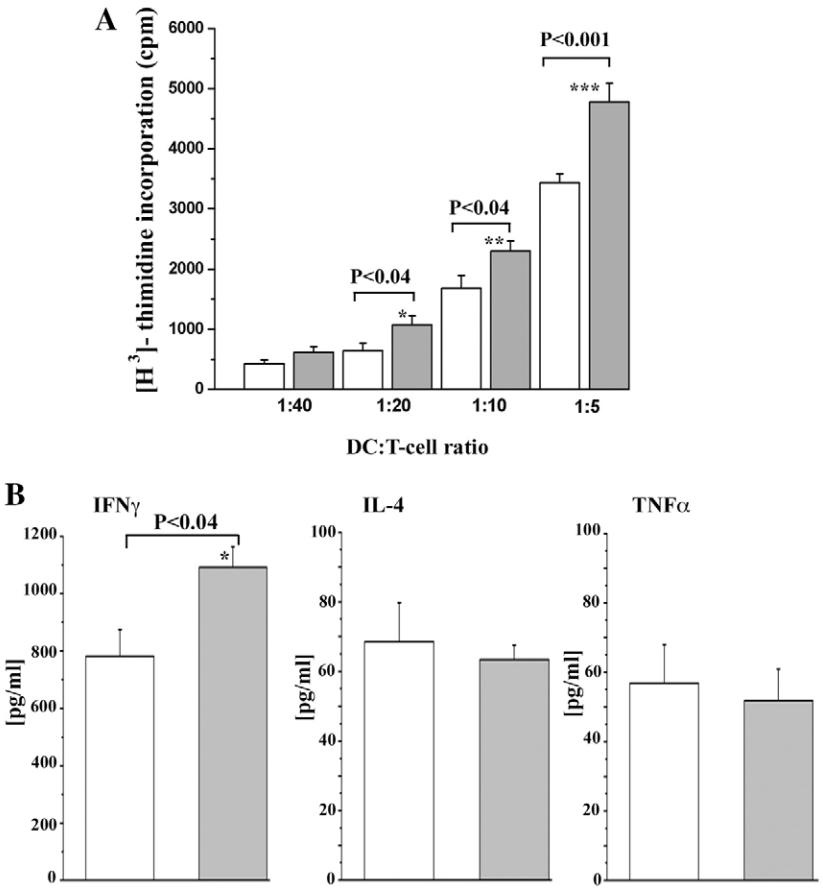

Fig. 2. DCs from HET RYR1$_{Y522S}$ mice are more efficient at stimulating T cells than their WT counterparts. (**A**) DCs were isolated from WT (white bars) and HET RYR1$_{Y522S}$ mice (grey bars) (C57BL/6) and cultured with allogenic CD4-positive T cells isolated from Balb/c mice as detailed in Materials and Methods, in graded DC to T-cell ratios. [^{3}H]thymidine incorporation from three different experiments carried out in triplicate is shown (mean±s.e.m.). (**B**) Analysis of cytokines released into the supernatant following the mixed lymphocyte reaction at a DC:T-cell ratio of 1:2.5 as detailed in Materials and Methods. T-cells incubated with HET RYR1$_{Y522S}$ DCs (grey bars) release significantly higher levels of IFNγ compared with T-cells incubated with WT DCs (white bars). Results are the mean±s.e.m. of three experiments carried out in triplicate.

amount of TNF-α, and IL-4 (Fig. 2B). No IL-10 was detected in the supernatants of the mixed lymphocyte reactions from either group (not shown).

Blood counts, immune cell subpopulations and natural Ig in non-challenged mice

The total number of circulating leukocytes, erythrocytes and reticulocytes were similar in WT and HET RYR1$_{Y522S}$ mice (supplementary material Table S1). There was a small but significant increase in the total number of circulating lymphocytes but close evaluation did not reveal any differences in the % CD4 or CD8 positive cells (not shown). Splenocytes isolated from HET RYR1$_{Y522S}$ and WT littermates were labelled with antibodies against CD4, CD8, CD3, CD19, MHCII, CD11c, CD11b and CD83 and the % positive cells was monitored by FACS. Supplementary material Fig. S1 shows that there was no significant difference in the % of DCs, B-lymphocytes and macrophages; there was a small but significant increase in CD3-positive T-cells (mean % ± s.e.m. was 29.4±0.78% vs 33.3±0.9% in 12 WT and 10 HET RYR1$_{Y522S}$ littermates, respectively $P<0.003$). A closer evaluation revealed that this is due to an increase in the % CD4-positive subpopulation (mean % ± s.e.m. were 54.8±0.4% and 58.7±0.5% $P<0.0001$ in WT and HET RYR1$_{Y522S}$ littermates, respectively). Spleen weights were similar in WT and HET RYR1$_{Y522S}$ littermates (mean ± s.e.m. weights were 93.1±4.8 and 100.6±4.8 mg, respectively).

When examining the levels of circulating immunoglobulins in non-immunized mice, we noticed that HET RYR1$_{Y522S}$ mice have significantly higher levels of natural IgG_1 and IgE compared to their WT littermates but show no significant differences in the levels of IgM, IgG_{2a}, IgG_{2b} or IgG_3 (Fig. 3). Such changes were not accompanied by changes in IL-4, IL-10 or IL-6 as the circulating levels of these cytokines remained undetectable in both mice groups. Surprisingly there were no changes in the population of splenic Th2 cells, as WT and HET RYR1$_{Y522S}$ mice showed similar levels of expression of the Th2-specific surface markers T1/ST2, OX40 and inducible T-cell co-stimulator (COS) (Clay et al., 2009; Withers et al., 2009). Furthermore no changes were observed in the levels of the Th1 and Th2 commitment transcription factors T-box expressed in T-cells (Tbet) and GATA-3 (Zhu et al., 2010) (supplementary material Table S2). In addition, no differences were found in the native spleen B-cell populations as determined by the expression of surface immunoglobulins (IgM, IgG_1, IgE), nor in the spleen populations of plasma cells, as determined by the expression of CD138 (supplementary material Table S2). Re-stimulation of splenic T-cells *in vitro* with CD3/CD28 beads did not reveal any difference between HET RYR1$_{Y522S}$ and WT T-helper cell commitment since intracellular cytokine staining related to Th1/Th2/Th17 profiles were not changed (supplementary material Table S2).

Enhanced humoral immune response in HET RYR1$_{Y522S}$ knock-in mice after antigenic challenge

Since HET RYR1$_{Y522S}$ knock-in mice express high levels of natural circulating immunoglubulins we investigated if they

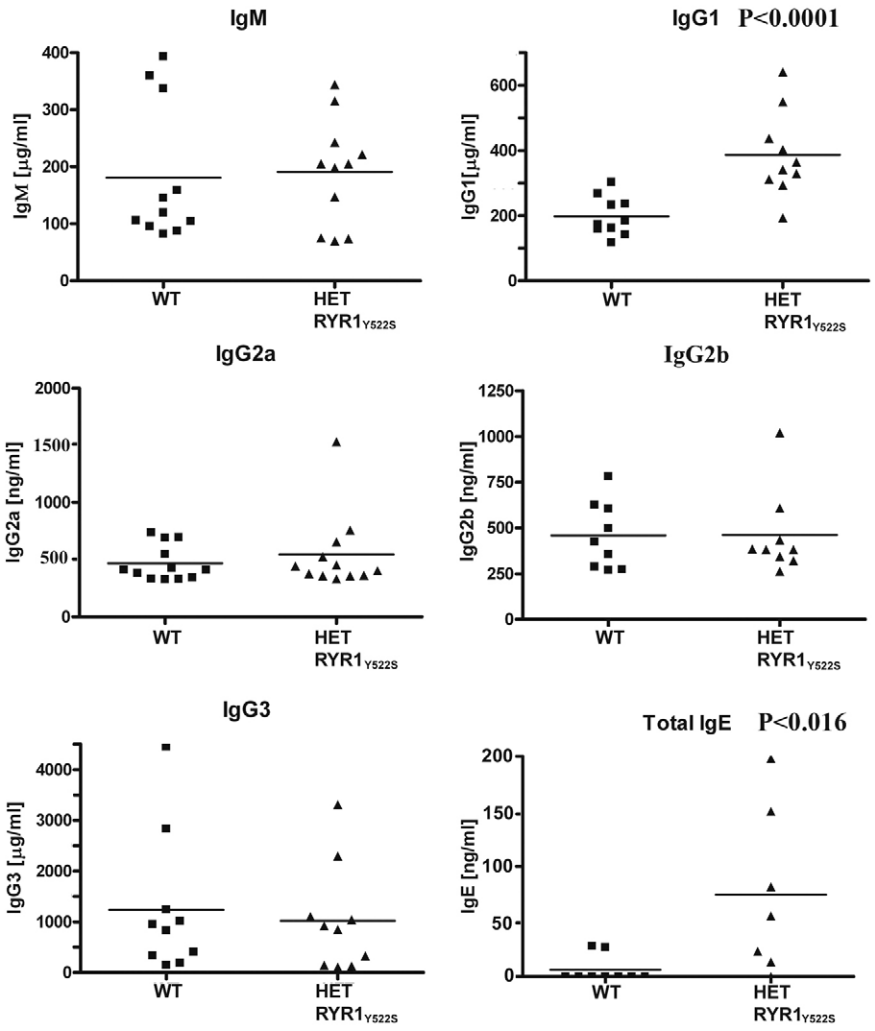

Fig. 3. Pre-immune serum IgG_1 and IgE levels are significantly higher in HET $RYR1_{Y522S}$ knock-in mice compared with those in their wild-type littermates. Mice were caged in the specific pathogen free facility of the ZLF of the Basel University Hospital; each point represents the concentration of the indicated immunoglobulin determined per mouse. WT mice, black boxes; HET $RYR1_{Y522S}$ knock-in mice, black triangles. *P*-values were significantly different according to the Student's *t*-test.

showed an enhanced immune response after an antigenic challenge. To this end we followed the immune response to (i) ovalbumin (OVA), a well-characterized antigen for studying murine immune functions, and (ii) *Heligmosomoides polygyrus (H.p.) bakeri*, a helminthic parasite. In the first case, mice were immunized intraperitoneally with different amounts of ovalbumin (10, 20, 50, 100 and 200 μg) and the serum levels of OVA-specific immunoglobulins were determined after 7, 14 and 21 days. Fig. 4A shows that after 7 days HET $RYR1_{Y522S}$ mice immunized with 100 μg OVA produced double the amount of OVA-specific IgG_1 than their WT littermates. With higher or lower concentrations of OVA IgG_1 levels were similar in WT and HET $RYR1_{Y522S}$ littermates (not shown). No significant differences were found in OVA-specific IgG_1 levels 14 and 21 days after the primary challenge (Fig. 4A).

Because HET RYR_{Y522S} mice have elevated natural IgE and because immune responses to helminthic infections preferentially elicit IgE responses, we challenged HET $RYR1_{Y522S}$ knock-in and control WT littermates to infection with *H.p. bakeri*. After 7 and 14 days, the serum was checked for parasite-specific antibodies and at 15 days the mice were sacrificed, the worm titre per mouse and white blood cell counts evaluated. No differences in the number or type of white blood cells were observed between WT and knock-in mice (supplementary material Table S3). Antibody titres to two worm-specific antigens were assessed by enzyme linked immunosorbent assay (ELISA) by monitoring reactivity against: (i) soluble extracts of whole worms and (ii) *H. p. bakeri* excretory-secretory (HES) Ag, a major target of the murine primary immune response. Fig. 4B and supplementary material Tables S4, S5 show that after 7 days there is a significant increase in parasite-specific IgG_1, both to whole worm extracts and to the HES Ag, in HET RYR_{Y522S} knock-in mice compared to WT littermates. At 14 days parasite-specific IgG_1 reach the same levels in WT and knock-in mice. No correlation was found between the titres of worm/HES-specific antibodies and worm load.

Discussion

A large number of studies have investigated the effects of *RYR1* mutations on muscle cell Ca^{2+} homeostasis but very little information is available concerning how such mutations affect other RyR1 expressing cells including immune cells. In this study we explored the consequences of the MHS-causative *RYR1* Y522S mutation by analysing the phenotypic and functional characteristics of DCs from HET $RYR1_{Y522S}$ mice as well as their immune response to antigenic challenges.

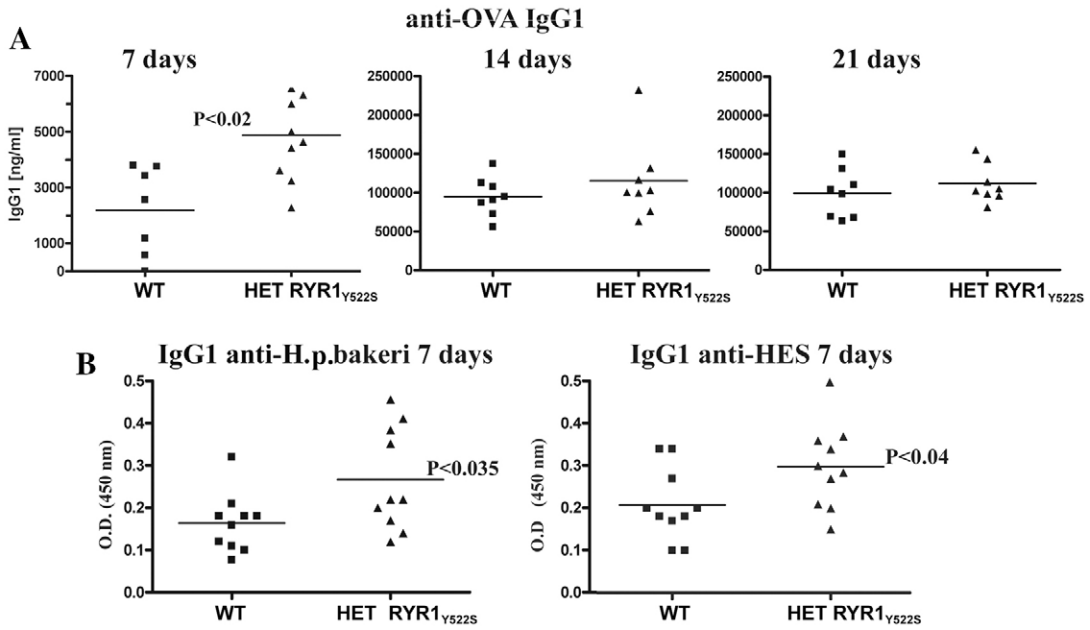

Fig. 4. HET $RYR1_{Y522S}$ knock-in mice produce higher titres of antigen-specific IgG_1 than their wild-type littermates at the early stages post-infection or immunization. (**A**) Mice were immunized with 100 µg OVA as described in Materials and Methods, and the concentration of circulating OVA-specific IgG_1 was determined after 7, 14 and 21 days. After 7 days the mice were re-immunized. Each point represents the average level of IgG_1 per mouse. WT mice, black boxes; HET $RYR1_{Y522S}$ knock-in mice, black triangles. The serum levels of anti-OVA IgG_1 are significantly higher in the HET $RYR1_{Y522S}$ mice. Statistical analysis was performed using the ANOVA test followed by the Bonferroni post hoc test (*P<0.02). (**B**) Mice were orally infected with *H. p. bakeri* larvae and the concentration of worm-specific (left panel) or HES-specific (right panel) IgG_1 was determined after 7 days by ELISA. Each point represents the average amount of IgG_1 per mouse. WT mice, black boxes; HET $RYR1_{Y522S}$ knock-in mice, black triangles. P-values were significantly different according to the Student's t-test.

Effect of the *RYR1* Y522S mutation on the unchallenged immune system

Splenic CD11c-positive DCs from the HET $RYR1_{Y522S}$ mice exhibit elevated resting Ca^{2+} levels, a result which is consistent with the finding that most dominant *RYR1* mutations linked to MHS cause an increase in the resting [Ca^{2+}] concentration in skeletal muscle cells and B-lymphocytes (Ducreux et al., 2004; López et al., 2005; Levano et al., 2009; Vukcevic et al., 2010). Thus we hypothesized that the HET $RYR1_{Y522S}$ knock-in mouse, which expresses a gain-of-function mutation (Chelu et al., 2006) would be a useful tool to study in depth the role(s) of RyR1-dependent signalling in the immune system. We first focused our efforts on identifying differences in the 'resting' characteristics of the immune system by analysing the phenotype of freshly isolated unchallenged DCs and levels of natural immunoglobulins and subsequently studied the animal's immune response to antigenic challenges. DCs isolated from the spleens of HET $RYR1_{Y522S}$ mice express higher levels of the maturation marker CD83 compared to their wild-type littermates, a result that is compatible with the finding that surface expression of CD83 is increased in mature human and murine DCs (Weissman et al., 1995; Zhou and Tedder, 1996; Berchtold et al., 1999; Kuwano et al., 2007). We have previously shown that in human DCs Ca^{2+} signals generated via RyR1 activation act synergistically with toll like receptors and induce DC maturation (Bracci et al., 2007) yet Stolk et al. (Stolk et al., 2006) reported that DCs isolated from WT and RyR1 knock-out mice exhibit similar capacities to mature, endocytose antigens and stimulate T-cell proliferation. We would like to point out that chronic depletion of a protein from birth can activate compensatory mechanisms and the results of the present study support the role(s) of RyR1-signalling in DC function.

We are aware that the change in CD83 expression observed in DCs from HET $RYR1_{Y522S}$ mice is equivalent to a 30% increase, however (i) we exclude that such a small difference is due to differences in the genetic background of wild-type and knock-in mice since the mice were backcrossed in the same mouse strain (C57BL/6) and all experiments were performed on littermates, so that the only difference between the mice is a mutation in the *RYR1* gene which causes increased agonist sensitivity and an increase in the cytoplasmic resting [Ca^{2+}] from ~50 nM to 125 nM, and (ii) the increase in CD83 expression is sufficient to cause a measurable change in function since in a mixed lymphocyte reaction, DCs from HET $RYR1_{Y522S}$ mice were more potent at stimulating T-cell proliferation and induced higher levels of IFN-γ release than was observed in T-cells stimulated with WT DCs. Since no increase in CD83 transcripts were observed, we suggest that the increase in CD83 surface expression in the HET $RYR1_{Y522S}$ mice is due to Ca^{2+}-dependent release from an internal pool. Indeed increased surface expression of CD83 in DCs from WT mice could be induced already 2 minutes after the addition of the RyR1 agonist caffeine. These results are in line with the finding that CD83 molecules recycle between endosomes and the cell surface (Klein et al., 2005); in endosomes they co-localize with MHC class II molecules and we have previously shown that pharmacological stimulation of RyR1 results in the rapid expression of pre-formed MHC class II molecules on the cell surface (Vukcevic et al., 2008). Taken together these results support the observations that DC maturation results from the convergence of different signals

arising from cytokine release, RyR1-activation and NFkB translocation (Bracci et al., 2007; Baeuerle and Henkel, 1994; Frantz et al., 1994).

An interesting observation concerning the role played by RyR1 in the immune system is that the sera of 'un-stimulated' HET $RYR1_{Y522S}$ mice show elevated levels of circulating natural IgG_1 and IgE. Natural antibodies are produced in the absence of external antigenic stimulation and are directed against a wide spectrum of self- and non-self antigens (Avrameas et al., 2007); their role is related to early protection against pathogens (Ochsenbein et al., 1999; Baumgarth et al., 2005; McCoy et al., 2006). On the other hand, high levels of IgEs in conjunction with increased levels of eosinophils are often seen in the circulation of allergic individuals and are thought to arise because T cells orient towards the Th2 phenotype (Yazdanbakhsh et al., 2002). Our results suggest that RyR1 signalling in DCs may affect Th-cell differentiation by influencing their development into Th1 or Th2 and/or Treg. However, no changes in the release of IL-4 and TNF-α were observed in the mixed lymphocyte reaction and IL-10 and IL-4 were not detected in the sera of either mouse group. Furthermore under basal conditions no shift in the T-cell profile was observed in the spleens of WT and HET $RYR1_{Y522S}$ mice when evaluated for expression of transcription factors and surface markers characteristic for Th1 or Th2 cells. Accordingly, additional signals besides changes in Ca^{2+} homeostasis are probably required for T-cell orientation and release of IgG_1/IgE by plasma cells may be controlled by several Th-dependent mechanisms.

HET $RYR1_{Y522S}$ mice respond faster to antigenic challenges

Our next question deals with the influence of altered Ca^{2+} signalling on the development of a specific humoral immune response. This was approached by immunizing mice either with the non-infectious agent ovalbumin or, in light of the elevated IgE levels, with the helminthic parasite *H. p. bakeri*. In both cases the levels of antigen-specific IgG_1 reached similar levels in WT and HET $RYR1_{Y522S}$ mice at 2 weeks or later; however, HET $RYR1_{Y522S}$ mice were more rapid at responding to antigenic challenges during the early phases, i.e. at 7 days, indicating that the gain of function of antigen-presenting cells brought about by the *RYR1* knock-in mutation, primes the immune system so that it is more efficient at responding in a specific and T-cell dependent way to antigenic challenges. Indeed anti-OVA IgM values were similar in WT and HET $RYR1_{Y522S}$ mice. In the case of the parasitic infection HET $RYR1_{Y522S}$ mice were also faster than WT littermates in responding to the infection and produced more parasite-specific IgG_1 antibodies both to whole worm extracts and to the HES antigen, even though they ultimately harboured the same level of parasite counts as their wild-type littermates. Vaccination with HES has been reported to confer protection to experimental infection with *H. p. backeri*, but of the various antibodies generated, those recognizing the VAL-1, VAL-2 and VAL-4 antigens are non-protective and possibly act as decoy molecules giving rise to an ineffective immune response (Hewitson et al., 2011). In this context it should be mentioned that the number of circulating eosinophils was similar in both mice; thus, since eosinophils are involved in killing helminths, the early development of specific IgG_1 is not sufficient to protect the host against this parasitic infection.

The main question underlying the experiments described in the present manuscript is whether or not gain-of-function mutations in the RyR1 Ca^{2+} channel offers, or not, a selective advantage to its host. The primary organ that is affected by mutations is skeletal muscle, and aside from rendering the muscle excitation-contraction machinery more excitable to low levels of stimulation, there seems to be no overt advantage. While investigating the relationship between MH and cytokines we found that the presence of MH-causing *RYR1* mutations is associated with a higher release of the pro-inflammatory cytokines IL-6 and IL-1 from cultured myotubes and B-lymphocytes (Girard et al., 2001; Ducreux et al., 2004). Furthermore in humans, but not in mice, circulating levels of IL-1 and IL-6 are significantly elevated in individuals bearing dominant *RYR1* mutations compared to control subjects (S.T., F.Z. and M.V., unpublished results), indicating a potential complex interplay between infection/inflammation/*RYR1* mutations.

In conclusion, this report provides evidence that HET $RYR1_{Y522S}$ mice carrying the *RYR1* mutation Y522S have a gain in immune functions. These experiments represent 'the proof of concept' that pharmacological activation of 'normal' RyR1 may enhance primary immune responses. These results also raise several potentially important scientific and medical issues, namely the possibility that individuals with a genetic predisposition to develop allergies, thus possessing a Th2 orientation (IgE, eosinophils, IL-4 and IL-10) may express gain of function polymorphic variants of *RYR1*. Since vaccination induces a primary immune response and DCs represent a key target for adjuvant activity an important focus for future research in the field of new vaccine and adjuvant development could target the skeletal muscle RyR1 in doing so however, one must keep in mind that the RyR1 is predominantly expressed in skeletal muscle and its pharmacological activation could lead to severe consequences from abnormal muscle contraction to full-blown MH-like episodes.

Materials and Methods

Mice

HET $RYR1_{Y522S}$ knock-in mice model were kindly provided by Prof. Susan L. Hamilton (Chelu et al., 2006). Mice were caged in the Specific Pathogen Free SPF facility of the ZLF of the Basel University hospital and all experiments were performed following the regulations of the local Kantonal authorities (animal permit no. 1728 and 1729, 2081). For all experiments 8–10-week-old male heterozygous (HET $RYR1_{Y522S}$) mice and their wild-type littermate same sex siblings were used. Mice were genotyped by PCR amplification of genomic DNA isolated from a biopsy using the following primers and conditions: F 5′-TCTCCCTGGTCCTGAATTGC-3′ and R 5′-AGCGTACAGCCACACCATTG-3′, 95℃ 3 min followed by 30 cycles 95℃ 30 sec, 54℃ 45 sec, 72℃ 45 sec and a final extension at 72℃ for 4 min. Genotyping was performed by restriction enzyme digestion of the amplified genomic DNA with BlpI restriction enzyme. DNA from WT mice (−/−) yields a band of about 700 bp, while digestion of the genomic DNA from HET $RYR1_{Y522S}$ mice (+/−) shows in addition to the band 700 bp, a band of 600 bp.

Isolation of DCs, T-cells and B-cells from mouse spleens

Single-cell suspensions were prepared from mouse spleens by enzymatic disaggregation using collagenase type I (Sigma chemicals, St. Louis, MO, USA, C0130) according to the magnetic cell sorting protocol (Miltenyi Biotech, Bergisch Gladbach, Germany). DCs, T-cells and B-cells were isolated by positive sorting using anti-CD11c, CD4 and CD19-coated magnetic MicroBeads (Miltenyi Biotech, Bergisch Gladbach, Germany), according to the manufacturer's instructions.

Resting $[Ca^{2+}]$

Measurements were performed on fura-2 (Invitrogen, Lucerne, Switzerland) loaded CD11c+ splenic DCs isolated from wild-type and HET $RYR1_{Y522S}$ knock-in mice, as previously described (Ducreux et al., 2004). Briefly, after loading, cells were rinsed, resuspended in Krebs-Ringer medium containing 2 mM $CaCl_2$ and allowed to adhere to poly-lysine treated glass coverslips. Online (340 nm, 380 nm, and ratio) measurements were recorded using a fluorescent Axiovert S100 TV

inverted microscope (Carl Zeiss, Jena, Germany) equipped with a 40×oil immersion Plan NeoFluar objective (0.17 NA) and filters (BP 340/380, FT 425, BP 500/530) and attached to a Cascade 128+ CCD camera. Cells were analyzed using Metamorph and the average pixel value for each cell was measured at excitation wavelengths of 340 and 380 nm, as previously described (Ducreux et al., 2004). Fura-2 fluorescent ratio signals were converted into [Ca^{2+}] using the Fura-2 Ca^{2+} imaging calibration kit from Molecular Probes (Invitrogen, Lucerne, Switzerland, catalogue N° F6774) following the manufacturer's instructions. Images of Fura-2 in the different buffers were acquired using a 40×oil immersion Plan NeoFluar objective (0.17 NA) and filters (BP 340/380, FT 425, BP 500/530) and attached to a Cascade 128+ CCD camera as described above for resting [Ca^{2+}] measurements.

Flow cytometry

Flow cytometry was performed as previously described (Vukcevic et al., 2008) using a FACSCalibur equipped with Cell Quest software (Becton Dickinson Pharmingen, Allschwil, Switzerland). Briefly, cells were washed and resuspended in phosphate buffered saline (PBS), and incubated for 30 minutes at 4°C in the presence of fluorochrome labeled commercial monoclonal antibodies against the following surface markers: CD83, CD3, CD19, CD11c, CD11b, CD4, CD8, CD138, IgG_1, IgM, IgE and I-Ab or isotype-matched controls (Becton Dickinson Pharmingen, Allschwil, Switzerland).

RT PCR

Total RNA was isolated from dendritic cells using RNAeasy kit from Qiagen and treated with deoxyribonuclease I (DNase I) (Invitrogen, Lucerne, Switzerland) to eliminate contaminant genomic DNA. After reverse transcription using 500 ng of RNA (high-capacity cDNA reverse transcription kit, Applied Biosystems, Forster City, CA, USA), cDNA was amplified by quantitative real-time PCR using SYBR Green technology (Fast SYBR Green Master Mix, Applied Biosystem, Forster Cita, CA, USA) and exon-intron junction-designed primers for TATA box binding protein, CD83, CD86, IL12p40 and IL23p19. Gene expression was normalized using self-TATA box binding protein as reference. The expression of RYR1 was investigated by semi-quantitative RT PCR. cDNA was amplified using primers and conditions as described in genotyping section. Amplified cDNA was digested with the restriction enzyme BlpI; cDNA from WT mice (−/−) yields a band of ~376 bp, while digestion of the cDNA from HET $RYR1_{Y522S}$ (+/−) shows bands of ~376 bp and 276 bp plus a band of 100 bp.

Mixed lymphocytes reaction assay and cytokine secretion

Mixed leukocytes cultures were set up in triplicate in 96-well flat-bottom microplates (Becton Dickinson Pharmingen, Allschwil, Switzerland) with graded ratios of DC:T cells (1:2.5, 1:5, 1:10, 1:20, 1:40, 1:80, 1:160) using DCs isolated from WT and HET $RYR1_{Y522S}$ littermates with the C57BL/6 background as stimulator cells and 5×10^4 T-cells as isolated from WT BALB/c mice (responder cells). Cultures were incubated for 4 days in RPMI medium supplemented with 10% foetal calf serum. During last 18 h of culture, [^{3}H]thymidine was added and lymphocyte proliferation was assessed by [^{3}H]-thymidine incorporation. For cytokine secretion, the supernatants from mixed lymphocyte cultures were collected after 3 days of co-culture and the concentrations of IFNγ, TNFα, IL-4 and IL-10 were evaluated by ELISA (eBioscience, Inc., Becton Dickinson Pharmingen, Allschwil, Switzerland) following manufacturer's instructions.

Immunoglobulin enzyme linked immunosorbent assay (ELISA)

Circulating levels of IgG_1, IgG_{2a}, IgG_{2b}, IgG_3, IgE and IgM were determined by a sandwich ELISA using goat anti-mouse IgG_1 (GeneTex Inc., catalogue number GTX29165), IgG2a (GeneTex Inc., catalogue number GTX29163), IgG2b (GeneTex Inc., catalogue number GTX29164) and IgG_3 (GeneTex Inc., catalogue number GTX77284) as coating antibodies and goat anti-mouse IgG peroxidase (Sigma, St Louis, MO, USA, catalogue number A2304) as a secondary Ab. In the case of IgE, plates were coated with goat anti-mouse IgE (SouthernBiotech, Birmingham, AL, USA, catalogue number 1110-01) and horseradish peroxidase conjugated goat anti-mouse IgE (SouthernBiotech, Birmingham, AL, USA, catalogue number 1110-05) were used for detection. As standards we used mouse IgG_1, IgG_{2a}, IgG_{2b}, IgG_3 isotype controls (GeneTex Inc.) and mouse IgE isotype control (Biolegend, San Diego, CA, USA). To detect total IgM we used the ELISA kit from eBioscience (catalogue number 88-50470) and followed the manufacturer's instructions. Sera were diluted from 1:10 to 1:50,000 depending on the immunoglobulin being investigated.

Immunization and assessment of OVA specific IgGs

Wild-type and HET $RYR1_{Y522S}$ knock-in mice were immunized with five different concentrations of ovalbumin (10, 20, 50, 100 and 200 µg in 0.2 ml mixture of PBS and Alum as an adjuvant) and the sera were obtained 7, 14 and 21 days after the immunization. In some cases mice were re-immunized after 7 days. The presence of OVA specific IgG, IgG_1, IgG_{2a} and IgE antibodies was determined by ELISA. Briefly, 96-well plates were coated with 100 µg/ml OVA overnight at 4°C. Wells were washed with phosphate buffer saline (PBS), blocked with blocking buffer (1:100 dilution blocking solution from Roche in PBS) for 2 h at room temperature. Serum samples were diluted with PBS, added to the plates and incubated overnight at 4°C. Plates were washed with PBS, incubated with horseradish peroxidase conjugated secondary antibodies (goat anti-mouse IgG, IgG_1, IgG_{2a} and IgE diluted 1:4000 in PBS) for 1 hour at room temperature. The reaction was developed using 3,3′,5,5′-tetramethylbenzidine followed by 0.16 M sulphuric acid as previously described (Ducreux et al., 2004) and the absorbance was monitored at 450 nm with a Synergy H1 ELISA reader (BioTek Instruments, GmbH).

Heligmosomoides polygyrus bakeri infection, worm count and measurements of IgGs against soluble extracts of whole worms *and H. p. bakeri* excretory-secretory (HES) Ag

8–10 week-old WT or HET $RYR1_{Y522S}$ knock-in mice were infected orally with 80 L3. Blood was taken 7 and 14 days after infection and blood cell counts were performed with an Advia 120 Haematology Analyzer using the Multispecies Software (Bayer, Leverkusen, Germany). For worm counts, mice were killed 14 days post-infection by CO_2 euthanasia. For necroscopic examination, the entire intestine was removed from each mouse, placed in a Petri dish and opened longitudinally. All worms were removed and counted. Excretory-secretory antigens from adult *H. p. bakeri* (HES) were prepared as previously described (Hewitson et al., 2011). Soluble extracts of adult worms were prepared by lysing worms in 50 mM HEPES pH 8.0, 1 mM EDTA, 140 mM KCl 0.5% NP-40 1% Triton X-100, 1% deoxycholate. After vortexing, the extracts were placed on a rotary shaker for 30 min shake and centrifuged at 10,000 ***g*** for 5 min. The supernatant (total soluble extract) was collected and the protein concentration measured using BCA protein assay kit according to the manufacturer's instructions (Thermo Scientific Inc.). Specific IgG and IgE antibodies in plasma were determined by ELISA in 96-well plates (COSTAR 9018) coated overnight at 4°C with 0.2 µg/well of total worm soluble extract or 0.4 µg/well of HES Ag in coating buffer (0.1 M Carbonate/Bicarbonate buffer, pH 9.6). Wells were washed, blocked with blocking buffer for 2 h at room temperature and processed as described above for anti-OVA IgG determination.

Blood samples

Blood was collected from WT and HET $RYR1_{Y522S}$ knock-in mice in microtainer coated with EDTA (Becton Dickinson Pharmingen, Allschwil, Switzerland) and diluted 1:4 in 0.9% Sodium Chloride solution; samples were analysed with an Advia 120 Haematology Analyzer using the Multispecies Software (Bayer, Leverkusen, Germany). Peripheral blood mononuclear cells were isolated from fresh blood by Ficoll density gradient centrifugation (Histopaque, catalogue number 1077, Sigma Chemicals, St Louis, MO, USA), washed once, resuspended in phosphate-buffered saline and incubated for 30 minutes at 4°C in the presence of fluorochrome labeled commercial monoclonal antibodies recognizing the following surface markers: CD4 and CD8 or isotype-matched controls (Becton Dickinson Pharmingen, Allschwil, Switzerland). The percentage of CD4-positive or CD8-positive cells was determined using a FACSCalibur instrument equipped with Cell Quest software (Becton Dickinson Pharmingen, Allschwil, Switzerland).

T helper cell profiling

Splenocytes were analyzed freshly or 5 days after stimulation (10^6 cells/ml) with CD3/CD28 coated Dynabeads (Invitrogen, Lucerne, Switzerland). For re-stimulation of T cells, Dynabeads were removed from the culture medium, cells were allowed to recover overnight and were then re-stimulated with CD3/CD28 coated Dynabeads in the presence of monensin (Becton Dickinson Pharmingen, Allschwil, Switzerland) for 6 h. Prior to fixation, cells were stained for viability with the LIVE/DEAD cell staining kit (Invitrogen, Lucerne, Switzerland) and surface staining was performed. For intracellular detection of cytokines and transcription factors the Becton Dickinson (Pharmingen, Allschwil, Switzerland) Cytofix/Cytoperm Kit was used. Non-specific binding of Fcγ II/III receptors was blocked with anti-CD16/CD32 antibodies. Cells were analyzed on a FACSCanto II (Becton Dickinson Pharmingen, Allschwil, Switzerland). The following antibodies were used: phycoerythrin/Cy7 anti-mouse IL-4 and allophycocyanin anti-mouse IL-17A (Biolegend Europe), Alexa-Fluor 700 anti-mouse IFN-γ (Becton Dickinson Pharmingen, Allschwil, Switzerland); phycoerythrin anti-mouse GATA-3, peridinin chlorophyll protein anti-mouse T-bet, allophycocyanin anti-mouse Rorγt, phycoerythrin anti-mouse ICOS, phycoerythrin anti-mouse OX40 and phycoerythrin anti-mouse IL-13 (eBioscience Inc.).

Statistical Analysis

Statistical analysis was performed using the Student's *t*-test; means were considered statistically significant when the $P<0.05$. When more than two groups were compared, analysis was performed by the ANOVA test followed by the Bonferroni post hoc test.

Acknowledgements

We thank Susan L. Hamilton for the HET $RYR1_{Y522S}$ knock-in mice and Renate Looser for help with the blood cell counts. We also

acknowledge the support of the Departments of Anesthesia and Surgery of the Basel University Hospital. The authors declare no competing financial interests.

Author contributions

M.V. designed and performed the experiments and analysed data; F.Z. helped design the experiments and analysed data; S.K. performed experiments and analysed data; D.A.T. designed experiments and analysed data, J.K. designed experiments and analysed data; R.M.M. designed experiments and analysed data; S.T. took care of conception and design of the experiments, collection and analysis of data, and drafting of the manuscript.

Funding

This work was supported by a grant from the Swiss national science foundation (SNF) [grant number 310030-129785 to S.T., and in part by post-doctoral fellowship grant DMS 2187 to M.V.]; and by the Wellcome Trust [grant number 090281 to R.M.M.]. Deposited in PMC for release after 6 months.

Supplementary material available online at
http://jcs.biologists.org/lookup/suppl/doi:10.1242/jcs.130310/-/DC1

References

Avrameas, S., Ternynck, T., Tsonis, I. A. and Lymberi, P. (2007). Naturally occurring B-cell autoreactivity: a critical overview. *J. Autoimmun.* **29**, 213-218.

Baeuerle, P. A. and Henkel, T. (1994). Function and activation of NF-kappa B in the immune system. *Annu. Rev. Immunol.* **12**, 141-179.

Banchereau, J., Briere, F., Caux, C., Davoust, J., Lebecque, S., Liu, Y. J., Pulendran, B. and Palucka, K. (2000). Immunobiology of dendritic cells. *Annu. Rev. Immunol.* **18**, 767-811.

Baumgarth, N., Tung, J. W. and Herzenberg, L. A. (2005). Inherent specificities in natural antibodies: a key to immune defense against pathogen invasion. *Springer Semin. Immunopathol.* **26**, 347-362.

Berchtold, S., Ogilvie, A. L., Bogdan, C., Mühl-Zürbes, P., Ogilvie, A., Schuler, G. and Steinkasserer, A. (1999). Human monocyte derived dendritic cells express functional P2X and P2Y receptors as well as ecto-nucleotidases. *FEBS Lett.* **458**, 424-428.

Bracci, L., Vukcevic, M., Spagnoli, G., Ducreux, S., Zorzato, F. and Treves, S. (2007). Ca^{2+} signaling through ryanodine receptor 1 enhances maturation and activation of human dendritic cells. *J. Cell Sci.* **120**, 2232-2240.

Chelu, M. G., Goonasekera, S. A., Durham, W. J., Tang, W., Lueck, J. D., Riehl, J., Pessah, I. N., Zhang, P., Bhattacharjee, M. B., Dirksen, R. T. et al. (2006). Heat- and anesthesia-induced malignant hyperthermia in an RyR1 knock-in mouse. *FASEB J.* **20**, 329-330.

Clay, C. A., Lehmer, E. M., Jeor, S. S. and Dearing, M. D. (2009). Sin nombre virus and rodent species diversity: a test of the dilution and amplification hypotheses. *PLoS ONE* **4**, e6467.

De Crescenzo, V., Fogarty, K. E., Lefkowitz, J. J., Bellve, K. D., Zvaritch, E., MacLennan, D. H. and Walsh, J. V., Jr (2012). Type 1 ryanodine receptor knock-in mutation causing central core disease of skeletal muscle also displays a neuronal phenotype. *Proc. Natl. Acad. Sci. USA* **109**, 610-615.

Ducreux, S., Zorzato, F., Müller, C., Sewry, C., Muntoni, F., Quinlivan, R., Restagno, G., Girard, T. and Treves, S. (2004). Effect of ryanodine receptor mutations on interleukin-6 release and intracellular calcium homeostasis in human myotubes from malignant hyperthermia-susceptible individuals and patients affected by central core disease. *J. Biol. Chem.* **279**, 43838-43846.

Frantz, B., Nordby, E. C., Bren, G., Steffan, N., Paya, C. V., Kincaid, R. L., Tocci, M. J., O'Keefe, S. J. and O'Neill, E. A. (1994). Calcineurin acts in synergy with PMA to inactivate I kappa B/MAD3, an inhibitor of NF-kappa B. *EMBO J.* **13**, 861-870.

Girard, T., Cavagna, D., Padovan, E., Spagnoli, G., Urwyler, A., Zorzato, F. and Treves, S. (2001). B-lymphocytes from malignant hyperthermia-susceptible patients have an increased sensitivity to skeletal muscle ryanodine receptor activators. *J. Biol. Chem.* **276**, 48077-48082.

Hewitson, J. P., Harcus, Y., Murray, J., van Agtmaal, M., Filbey, K. J., Grainger, J. R., Bridgett, S., Blaxter, M. L., Ashton, P. D., Ashford, D. A. et al. (2011). Proteomic analysis of secretory products from the model gastrointestinal nematode Heligmosomoides polygyrus reveals dominance of venom allergen-like (VAL) proteins. *J. Proteomics* **74**, 1573-1594.

Klein, E., Koch, S., Borm, B., Neumann, J., Herzog, V., Koch, N. and Bieber, T. (2005). CD83 localization in a recycling compartment of immature human monocyte-derived dendritic cells. *Int. Immunol.* **17**, 477-487.

Kuwano, Y., Prazma, C. M., Yazawa, N., Watanabe, R., Ishiura, N., Kumanogoh, A., Okochi, H., Tamaki, K., Fujimoto, M. and Tedder, T. F. (2007). CD83 influences cell-surface MHC class II expression on B cells and other antigen-presenting cells. *Int. Immunol.* **19**, 977-992.

Levano, S., Vukcevic, M., Singer, M., Matter, A., Treves, S., Urwyler, A. and Girard, T. (2009). Increasing the number of diagnostic mutations in malignant hyperthermia. *Hum. Mutat.* **30**, 590-598.

López, J. R., Linares, N., Pessah, I. N. and Allen, P. D. (2005). Enhanced response to caffeine and 4-chloro-m-cresol in malignant hyperthermia-susceptible muscle is related in part to chronically elevated resting $[Ca^{2+}]_i$. *Am. J. Physiol. Cell Physiol.* **288**, C606-C612.

McCoy, K. D., Harris, N. L., Diener, P., Hatak, S., Odermatt, B., Hangartner, L., Senn, B. M., Marsland, B. J., Geuking, M. B., Hengartner, H. et al. (2006). Natural IgE production in the absence of MHC Class II cognate help. *Immunity* **24**, 329-339.

O'Connell, P. J., Klyachko, V. A. and Ahern, G. P. (2002). Identification of functional type 1 ryanodine receptors in mouse dendritic cells. *FEBS Lett.* **512**, 67-70.

Ochsenbein, A. F., Fehr, T., Lutz, C., Suter, M., Brombacher, F., Hengartner, H. and Zinkernagel, R. M. (1999). Control of early viral and bacterial distribution and disease by natural antibodies. *Science* **286**, 2156-2159.

Robinson, R., Carpenter, D., Shaw, M. A., Halsall, J. and Hopkins, P. (2006). Mutations in RYR1 in malignant hyperthermia and central core disease. *Hum. Mutat.* **27**, 977-989.

Sei, Y., Gallagher, K. L. and Basile, A. S. (1999). Skeletal muscle type ryanodine receptor is involved in calcium signaling in human B lymphocytes. *J. Biol. Chem.* **274**, 5995-6002.

Stolk, M., Leon-Ponte, M., Merrill, M., Ahern, G. P. and O'Connell, P. J. (2006). IP3Rs are sufficient for dendritic cell Ca^{2+} signaling in the absence of RyR1. *J. Leukoc. Biol.* **80**, 651-658.

Treves, S., Jungbluth, H., Muntoni, F. and Zorzato, F. (2008). Congenital muscle disorders with cores: the ryanodine receptor calcium channel paradigm. *Curr. Opin. Pharmacol.* **8**, 319-326.

Uemura, Y., Liu, T. Y., Narita, Y., Suzuki, M., Ohshima, S., Mizukami, S., Ichihara, Y., Kikuchi, H. and Matsushita, S. (2007). Identification of functional type 1 ryanodine receptors in human dendritic cells. *Biochem. Biophys. Res. Commun.* **362**, 510-515.

Vukcevic, M., Spagnoli, G. C., Iezzi, G., Zorzato, F. and Treves, S. (2008). Ryanodine receptor activation by Ca v 1.2 is involved in dendritic cell major histocompatibility complex class II surface expression. *J. Biol. Chem.* **283**, 34913-34922.

Vukcevic, M., Broman, M., Islander, G., Bodelsson, M., Ranklev-Twetman, E., Müller, C. R. and Treves, S. (2010). Functional properties of RYR1 mutations identified in Swedish patients with malignant hyperthermia and central core disease. *Anesth. Analg.* **111**, 185-190.

Weissman, D., Li, Y., Ananworanich, J., Zhou, L. J., Adelsberger, J., Tedder, T. F., Baseler, M. and Fauci, A. S. (1995). Three populations of cells with dendritic morphology exist in peripheral blood, only one of which is infectable with human immunodeficiency virus type 1. *Proc. Natl. Acad. Sci. USA* **92**, 826-830.

Withers, D. R., Jaensson, E., Gaspal, F., McConnell, F. M., Eksteen, B., Anderson, G., Agace, W. W. and Lane, P. J. (2009). The survival of memory CD4+ T cells within the gut lamina propria requires OX40 and CD30 signals. *J. Immunol.* **183**, 5079-5084.

Yazdanbakhsh, M., Kremsner, P. G. and van Ree, R. (2002). Allergy, parasites, and the hygiene hypothesis. *Science* **296**, 490-494.

Zhou, L. J. and Tedder, T. F. (1996). CD14+ blood monocytes can differentiate into functionally mature CD83+ dendritic cells. *Proc. Natl. Acad. Sci. USA* **93**, 2588-2592.

Zhu, J., Yamane, H. and Paul, W. E. (2010). Differentiation of effector CD4 T cell populations (*). *Annu. Rev. Immunol.* **28**, 445-489.

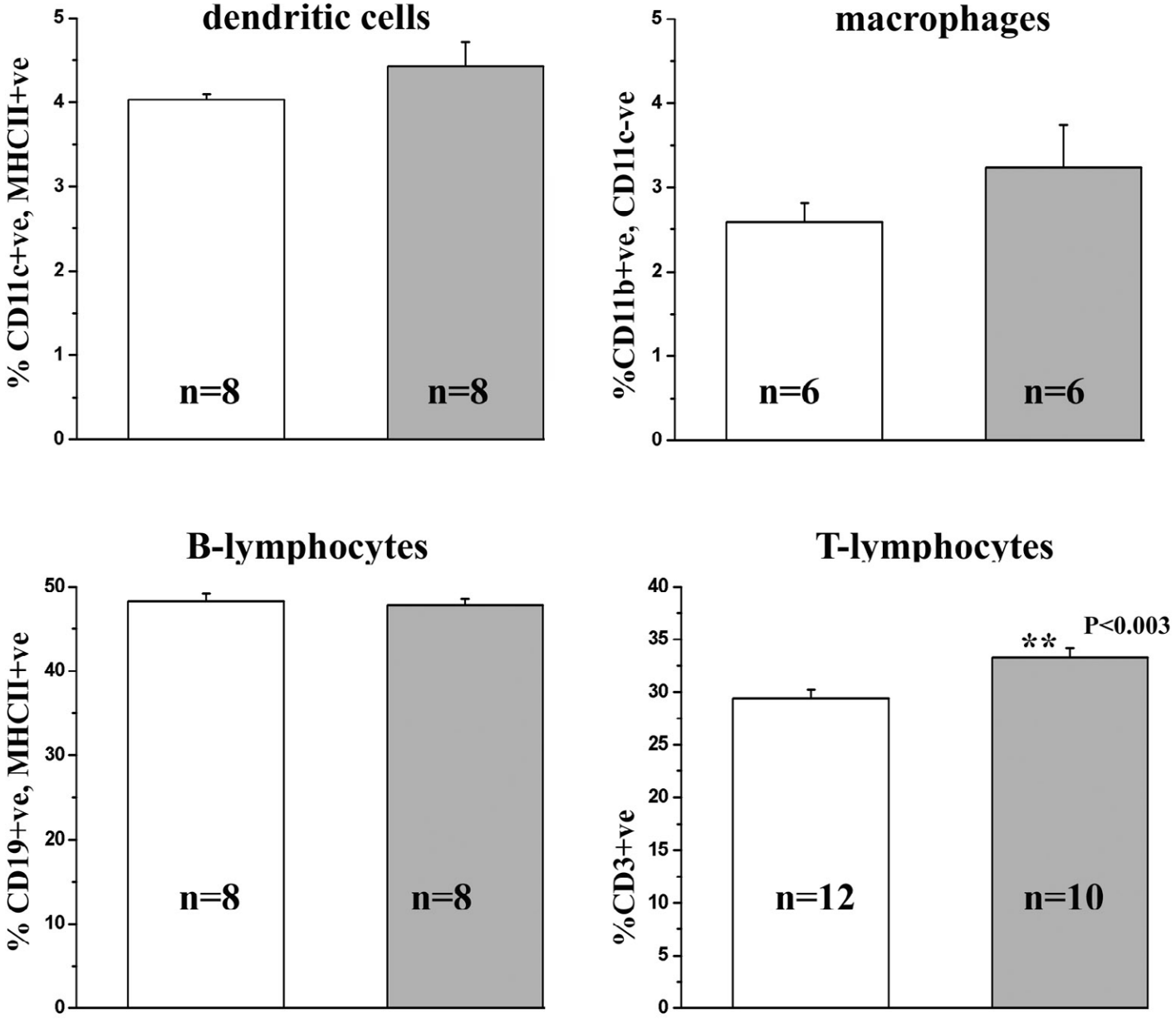

Fig. S1. The spleens isolated from HET RYR1$_{Y522S}$ mice contain a significantly higher percentage of CD3-positive T-cells, than the spleens of their WT littermates. Splenocytes isolated from WT and HET RYR1$_{Y522S}$ littermates were labelled with antibodies against CD4, CD8, CD3, MHCII, CD11c, CD11b and CD83 and the percentage of positive cells was monitored by FACS as described in the Methods section. Bars represent the mean (±s.e.m) percentage positive cells of experiments carried out in duplicate on the spleens isolated from n mice. The percentage of CD3-positive T-lymphocytes was significantly higher in HET RYR1$_{Y522S}$ mice compared to their WT littermates (P<0.003 Student's t test).

	WT (n=9)	**HET $RYR1_{Y522S}$ (n=10)**	**Significance**
Total leukocytes	10.44 ± 0.87 $x10^9$ /L	12.24 ± 2.6 $x10^9$ /L	N.S.
Neutrophils	1.02 ± 0.74 x 10^9 /L	1.11± 0.74 x 10^9 /L	N.S.
Lymphocytes	8.84 ± 1.44 x 10^9 /L	10.81± 2.27 x 10^9 /L	P< 0.04
Monocytes	0.15± 0.1 x 10^9 /L	0.12± 0.07x 10^9 /L	N.S.
Eosinophils	0.41± 0.29 x 10^9 /L	0.31± 0.07x 10^9 /L	N.S.
Platelets	1.60 ± 0.28 x 10^{12}/L	1.57 ± 0.21 x 10^{12}/L	N.S.
Erythrocytes	1.07± 0.6 x 10^{12}/L	1.13 ± 0.6 x 10^{12}/L	N.S.
Reticulocytes	3.34 ± 0.05 x 10^{12}/L	3.40 ±0.06 x 10^{12}/L	N.S.
Haematochrit	0.52 ±0.02 L/L	0.54 ±0.02L/L	P<0.05
Haemoglobin	154.7±9.8 g/L	159.6±3.5 g/L	N.S.

Table S1. Complete blood counts of WT and HET $RYR1_{Y522S}$ mice.

	T-cells					**B-cells**			
Mouse genotype	% of T1/ST2+ (mean±S.E.M)	% of OX40+ (mean±S.E.M)	% of ICOS+ (mean±S.E.M)	% of GATA3+ (mean±S.E.M)	% of Tbet+ (mean±S.E.M)	% of CD138+ (mean±S.E.M)	% of IgM+ (mean±S.E.M)	% of IgG1+ (mean±S.E.M)	% of IgE+ (mean±S.E.M)
WT	1.4±0.2	1.85±0.24	12.6±0.8	3.3±0.09	10.5±1.1	0.4±0.01	0.77±0.05	0.1±0.03	0.53±0.19
HET $RYR1_{Y522S}$	1.7±0.2	2.28±0.15	13.9±0.4	3.2±0.25	12.8±0.6	0.41±0.04	1.5±0.5	0.09±0.03	0.55±0.17

	T-cells after stimulation with CD3/CD28 beads Th1/Th2 cytokine profile				
Mouse genotype	% of CD44 (mean±S.E.M)	% of IFN-g (mean±S.E.M)	% of IL4 (mean±S.E.M)	% of IL13 (mean±S.E.M)	% of IL17 (mean±S.E.M)
WT	52.7±0.44	10.15±1.3	0.30±0.06	0.62±0.02	0.20±0.05
HET $RYR1_{Y522S}$	52.0±2.20	9.55±1.5	0.33±0.07	0.48±0.07	0.08±0.04

Table S2. T-helper and B-cell populations in the spleens of WT and HET $RYR1_{Y522S}$ mice.

Table S3: **Complete blood counts of WT and HET RYR1$_{Y522S}$ mice 7 and 14 days post *H.p. bakeri* infection**

7 days post infection	**WT (n=10)**	**HET RYR1$_{Y522S}$ (n=10)**	**Significance**
Total leukocytes	10.6 ± 5.9x 10^9 /L	8.2± 3.9 x 10^9 /L	n.s.
Neutrophils	5.0 ± 4.9 x 10^9 /L	3.4 ± 3.5 x 10^9 /L	n.s..
Lymphocytes	5.1 ± 1.7 x 10^9 /L	4.2 ± 1.9 x 10^9 /L	n.s.
Monocytes	0.2 ± 0.1 x 10^9 /L	0.2 ± 0.1 x 10^9 /L	n.s.
Eosinophils	0.3 ± 0.1 x 10^9 /L	0.4 ± 0.3 x 10^9 /L	n.s..
Platelets	1.5 ± 0.3 x 10^{12} /L	1.4 ± 0.1 x 10^{12} /L	n.s.
Erythrocytes	10.6 ± 5.5 x 10^{12} /L	10.1 ± 4.5 x 10^{12} /L	n.s.
Reticulocytes	3.4 ± 0.9 x 10^{12} /L	2.6 ± 0.5 x 10^{12} /L	P<0.03
Haematocrit	0.49 ± 0.03 L /L	0.50 ± 0.02 L /L	n.s.
Haemoglobin	150.0 ± 9.2 g/L	153.2 ± 5.7 g/L	n.s.
14 days post infection			
Total leukocytes	10.1 ± 2.9 x10^9 /L	9.6 ± 3.7 x10^9 /L	n.s.
Neutrophils	1.6 ± 1.1 x 10^9 /L	2.4 ± 2.8 x 10^9 /L	n.s..
Lymphocytes	7.7 ± 2.5 x 10^9 /L	6.3 ± 1.7 x 10^9 /L	n.s.
Monocytes	0.20 ± 0.1x 10^9 /L	0.20 ± 0.1 x 10^9 /L	n.s.
Eosinophils	0.6 ± 0.20 x 10^9 /L	0.6 ± 0.3 x 10^9 /L	n.s..
Platelets	1.6 ± 0.3 x 10^{12} /L	1.6 ± 0.2 x 10^{12} /L	n.s.
Erythrocytes	9.6 ± 0.6 x 10^{12} /L	9.6 ± 0.5 x 10^{12} /L	n.s.
Reticulocytes	7.6 ± 0.8 x 10^{12} /L	7.4 ± 0.9 x 10^{12} /L	n.s.
Haematocrit	0.45 ± 0.02 L /L	0.45 ± 0.03 L /L	n.s.

Table S3. Complete blood counts of WT and HET RYR1$_{Y522S}$ mice 7 and 14 days post *Heligmosomoides polygyrus bakeri* infection.

Mouse N°	**genotype**	**Anti-*H.p.bakeri*** IgG_1 7 days	**Anti-HES** IgG_1 7 days	**Anti-*H.p.bakeri*** IgG_1 14 days	**Anti-HES** IgG_1 14 days	**Anti-*H.p.bakeri*** IgE 14 days	**Anti-HES** IgE 14 days	***H.p.bakeri*** **Worm load**
940	WT	0.159	0.34	0.31	1.10	0. 098	0.33	11
982	WT	0.18	0.20	0.42	1.20	0.03	0.23	20
956	WT	0.11	0.18	0.70	1.20	0.014	0.16	81
991	WT	0.18	0.27	0.40	1.30	0.09	0.20	21
948	WT	0.21	0.18	0.50	0.90	-	0.22	56
987	WT	0.1	0.10	0.41	1.10	0.02	0.27	5
950	WT	0.32	0.34	0.34	0.52	0.01	0.12	20
937	WT	0.18	0.20	0.67	1.40	0.024	0.22	24
965	WT	0.1	0.17	0.43	0.90	0.004	0.20	16
949	WT	0.077	0.10	0.40	0.90	0.02	0.17	19
939	HET	0.20	0.29	0.80	1.54	0.11	0.43	19
983	HET	0.46	0.37	0.34	0.56	0.005	0.14	4
930	HET	0.41	0.50	0.80	0.90	-	0.23	5
957	HET	0.17	0.21	0.31	0.65	0.013	0.21	10
988	HET	0.35	0.36	0.60	1.20	0.02	0.35	23
989	HET	0.14	0.20	0.40	0.60	0.024	0.26	9
990	HET	0.22	0.27	1.10	2.80	0.03	0.16	81
951	HET	0.12	0.15	0.40	0.85	0.014	0.25	27
938	HET	0.38	0.30	0.71	1.75	0	0.37	82

Table S4. Ig against total *Heligmosomoides polygyrus bakeri* extract and HES and *Heligmosomoides polygyrus bakeri* worm load after 7 and 14 days in WT and HET $RYR1_{Y522S}$ mice.

Table S5: Mean (±SEM) anti-*H. p. bakeri* and anti-HES Ig titers in WT and HET $RYR1_{Y522S}$ mice.

	Whole worm protein extract				**HES**				
Mouse genotype	**IgG_1 7 days**	**IgG_1 14 days**	**IgE 7 days (**	**IgE 14 days**	**IgG_1 7 days**	**IgG_1 14 days**	**IgE 7 days**	**IgE 14 days**	**Worm count**
WT	0.162±0.02	0.458±0.04	#n.d.	0.034±0.01	0.208±0.03	1.05±0.08	#n.d.	0.21±0.01	27.3±7.3
HET $RYR1_{Y522S}$	*0.267±0.04	0.607±0.08	#n.d.	0.027±0.01	**0.299±0.03	1.27±0.20	#n.d.	0.26±0.03	31.5±9.6

*P<0.035 Student's t test
**P<0.04
not detected

Table S5. Mean (± SEM) anti-*Heligmosomoides polygyrus bakeri* and anti-HES Ig titers in WT and HET $RYR1_{Y522S}$ mice.